On the Ill-Posedness of Certain Vehicular Platoon Control Problems

Mihailo R. Jovanović, *Member, IEEE,* and Bassam Bamieh, *Senior Member, IEEE*

***Abstract*—We revisit the vehicular platoon control problems formulated by Levine and Athans and Melzer and Kuo. We show that in each case, these formulations are effectively ill-posed. Specifically, we demonstrate that in the first formulation, the system's stabilizability degrades as the size of the platoon increases, and that the system loses stabilizability in the limit of an infinite number of vehicles. We show that in the LQR formulation of Melzer and Kuo, the performance index is not detectable, leading to nonstabilizing optimal feedbacks. Effectively, these closed-loop systems do not have a uniform bound on the time constants of all vehicles. For the case of infinite platoons, these difficulties are easily exhibited using the theory of spatially invariant systems. We argue that the infinite case is a useful paradigm to understand large platoons. To this end, we illustrate how stabilizability and detectability degrade as functions of a finite platoon size, implying that the infinite case is an idealized limit of the large, but finite case. Finally, we show how to pose $\mathcal{H}_2$ and $\mathcal{H}_\infty$ versions of these problems where the detectability and stabilizability issues are easily seen, and suggest a well-posed alternative formulation based on penalizing absolute positions errors in addition to relative ones.**

***Index Terms*—Optimal control, spatially invariant systems, Toeplitz and circulant matrices, vehicular platoons.**

I. Introduction

In THIS paper, we consider optimal control of vehicular platoons. This problem was originally studied by Levine and Athans [1], and for an infinite string of moving vehicles by Melzer and Kuo [2], both using linear quadratic regulator (LQR) methods. We analyze the solutions to the LQR problem provided by these authors as a function of the size of the formation, and show that these control problems become effectively ill-posed as the size of the platoon increases. We investigate various ways of quantifying this ill-posedness. In Section II, we show that essentially, the resulting closed-loop systems do not have a uniform bound on the rate of convergence of the regulated states to zero. In other words, as the size of the platoon increases, the closed-loop system has eigenvalues that limit to the imaginary axis.

In Section II, we setup the problem formulations of [1] and [2] and investigate the aforementioned phenomena for finite platoons both numerically and analytically. In Section III, we also consider the infinite platoon case as an insightful limit which can be treated analytically. We argue that the infinite platoons capture the essence of the large-but-finite platoons. The infinite problem is also more amenable to analysis using the theory for spatially invariant linear systems [3], which we employ to show that the original solutions to this problem are not exponentially stabilizing in the case of an infinite number of vehicles. The reason for this is the lack of stabilizability or detectability of an underlying system. Thus, these control problems are inherently ill-posed even if methods other than LQR are used. In Section IV, we suggest alternative problem formulations which are well-posed. The main feature of these alternative formulations is the addition of penalties on absolute position errors in the performance index. Well-posed LQR, $\mathcal{H}_2$, and $\mathcal{H}_\infty$ problem formulations for infinite strings are proposed. In Section V, we consider a platoon of vehicles arranged in a circle, which is an idealization of the case of equally spaced vehicles on a closed track. For a spatially invariant LQR problem, we investigate whether one can impose uniform bounds on the convergence rates by appropriate selection of state and control penalties. We show that in the formulation of Levine and Athans [1] this is possible at the expense of using a high-gain feedback. Specifically, the feedback gains increase with the size of the platoon and they grow unboundedly in the limit of an infinite number of vehicles. We end our presentation with some concluding remarks in Section VI.

Manuscript received November 24, 2003; revised February 25, 2005 and May 31, 2005. Recommended by Associate Editor E. Jonckheere. This work was supported in part by the Air Force Office of Scientific Research under Grant FA9550-04-1-0207 and by the National Science Foundation under Grant ECS-0323814.

M. R. Jovanović is with the Department of Electrical and Computer Engineering, the University of Minnesota, Minneapolis, MN 55455, USA (e-mail: mihailo@umn.edu).

B. Bamieh is with the Department of Mechanical Engineering, University of California, Santa Barbara, CA 93106 USA (e-mail: bamieh@engineering.ucsb.edu).

Digital Object Identifier 10.1109/TAC.2005.854584

II. Optimal Control of Finite Platoons

In this section, we consider the LQR problem for finite vehicular platoons. This problem was originally studied by Levine and Athans [1] and subsequently by Melzer and Kuo [2], [4]. The main point of our study is to analyze the control strategies of [1], [2], and [4] as the number of vehicles in platoon increases. We show that the solutions provided by these authors yield the nonuniform rates of convergence toward the desired formation. In other words, we demonstrate that the time constant of the closed-loop system gets larger as the platoon size increases.

A. Problem Formulation

A system of M identical unit mass vehicles is shown in Fig. 1. The dynamics of this system can be obtained by representing each vehicle as a moving mass with the second-order dynamics

$$\ddot{x}_n + \kappa \dot{x}_n = u_n, \qquad n \in \{1, \ldots, M\} \tag{1}$$

where x_n represents the position of the nth vehicle, u_n is the control applied on the nth vehicle, and $\kappa \geq 0$ denotes the linearized drag coefficient per unit mass.

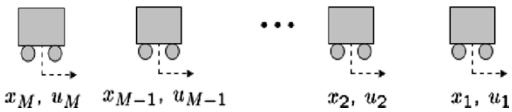

Fig. 1. Finite platoon of vehicles.

A control objective is to provide the desired cruising velocity v_d and to keep the distance between neighboring vehicles at a constant prespecified level δ. By introducing the absolute position and velocity error variables

$$\xi_n(t) := x_n(t) - v_d t + n\delta \qquad n \in \{1,\ldots,M\}$$
$$\zeta_n(t) := \dot{x}_n(t) - v_d, \qquad n \in \{1,\ldots,M\}$$

system (1) can be rewritten using a state–space realization of the form [2], [4]

$$\begin{bmatrix}\dot{\xi}\\ \dot{\zeta}\end{bmatrix} = \begin{bmatrix}0 & I\\ 0 & -\kappa I\end{bmatrix}\begin{bmatrix}\xi\\ \zeta\end{bmatrix} + \begin{bmatrix}0\\ I\end{bmatrix}\tilde{u} =: A\psi + B\tilde{u} \tag{2}$$

where $\xi := [\xi_1 \cdots \xi_M]^*, \zeta := [\zeta_1 \cdots \zeta_M]^*, \tilde{u} := [\tilde{u}_1 \cdots \tilde{u}_M]^*$, and $\tilde{u}_n := u_n - \kappa v_d$. Alternatively, by introducing the relative position error variable

$$\eta_n(t) := x_n(t) - x_{n-1}(t) + \delta = \xi_n(t) - \xi_{n-1}(t)$$

for every $n \in \{2,\ldots,M\}$, and neglecting the position dynamics of the first vehicle, the system under study can be represented by a realization with $2M-1$ state–space variables [1]

$$\begin{bmatrix}\dot{\eta}\\ \dot{\zeta}\end{bmatrix} = \begin{bmatrix}0 & \bar{A}_{12}\\ 0 & -\kappa I\end{bmatrix}\begin{bmatrix}\eta\\ \zeta\end{bmatrix} + \begin{bmatrix}0\\ I\end{bmatrix}\tilde{u} =: \bar{A}\phi + \bar{B}\tilde{u} \tag{3}$$

with $\eta := [\eta_2 \ldots \eta_M]^*$, and $\bar{A}_{12}$ being an $(M-1)\times M$ Toeplitz matrix with the elements on the main diagonal and the first upper diagonal equal to -1 and 1, respectively.

Following [2] and [4], fictitious lead and follow vehicles, respectively indexed by 0 and $M+1$, are added to the formation (see Fig. 2). These two vehicles are constrained to move at the desired velocity v_d and the relative distance between them is assumed to be equal to $(M+1)\delta$ for all times. In other words, it is assumed that

$$\{x_0(t) = v_d t, x_{M+1}(t) = v_d t - (M+1)\delta \qquad \forall\, t \geq 0\}$$

or, equivalently

$$\left.\begin{array}{lllll}\xi_0(t) & = & \xi_{M+1}(t) & = & 0\\ \zeta_0(t) & = & \zeta_{M+1}(t) & = & 0\end{array}\right\} \qquad \forall\, t \geq 0. \tag{4}$$

A performance index of the form [2], [4]

$$J := \frac{1}{2}\int_0^\infty \sum_{n=1}^{M+1} q_1(\xi_n(t) - \xi_{n-1}(t))^2\,\mathrm{d}t + \frac{1}{2}\int_0^\infty \sum_{n=1}^{M}\left(q_3\zeta_n^2(t) + r\tilde{u}_n^2(t)\right)\,\mathrm{d}t \tag{5}$$

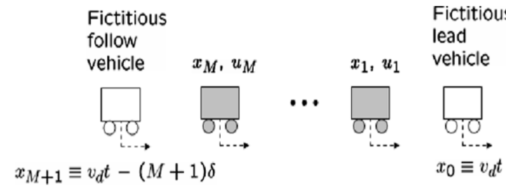

Fig. 2. Finite platoon with fictitious lead and follow vehicles.

is associated with (2). Using (4), J can be equivalently rewritten as

$$J = \frac{1}{2}\int_0^\infty (\psi^*(t)Q\psi(t) + \tilde{u}^*(t)R\tilde{u}(t))\,\mathrm{d}t$$

where matrices Q and R are determined by

$$Q := \begin{bmatrix}Q_1 & 0\\ 0 & q_3 I\end{bmatrix} \quad Q_1 := q_1 T_M \quad R := rI$$

with T_M being an $M \times M$ symmetric Toeplitz matrix with the first row given by $[2\ {-1}\ 0 \cdots 0] \in \mathbb{R}^M$. The control problem is now in the standard LQR form.

On the other hand, Levine and Athans [1] studied the finite string of M vehicles shown in Fig. 1, with state–space representation (3) expressed in terms of the relative position and absolute velocity error variables. In particular, the LQR problem with a quadratic performance index

$$J := \frac{1}{2}\int_0^\infty \left(\sum_{n=2}^{M} q_1\eta_n^2(t) + \sum_{n=1}^{M}\left(q_3\zeta_n^2(t) + r\tilde{u}_n^2(t)\right)\right)\,\mathrm{d}t \tag{6}$$

was formulated. Furthermore, the solution was provided for a platoon with $M = 3$ vehicles and $\{\kappa = r = 1, q_1 = 10, q_3 = 0\}$. We take a slightly different approach and analyze the solution to this problem as a function of the number of vehicles in platoon.

B. Numerical Results

1) Melzer and Kuo [4]: The top left and top right plots in Fig. 3 respectively show the dependence of the minimal and maximal eigenvalues of the solution to the LQR algebraic Riccati equation (ARE) P_M for system (2) with performance index (5), for $\{\kappa = 0, q_1 = q_3 = r = 1\}$. Clearly, $\lambda_{\min}\{P_M\}$ decays monotonically toward zero indicating that the pair (Q, A) gets closer to losing its detectability as the number of vehicles increases. This also follows from the Popov–Belevitch–Hautus (PBH) detectability test. Namely, as illustrated in the top left plot of Fig. 5, the minimal singular values of $D_M(\lambda) := [A^T - \lambda I\ Q^T]^T$ at $\lambda = 0$ decrease monotonically with M. On the other hand, $\lambda_{\max}\{P_M\}$ converges toward the constant value that determines the optimal value of cost functional (5) as M goes to infinity. The bottom plot in Fig. 3 illustrates the location of the dominant poles of system (2) connected in feedback with a controller that minimizes cost functional (5) for $\{\kappa = 0, q_1 = q_3 = r = 1\}$. The dotted line represents the function $-3.121/M$ which indicates that the least-stable eigenvalues of the closed-loop A-matrix approximately scale in an

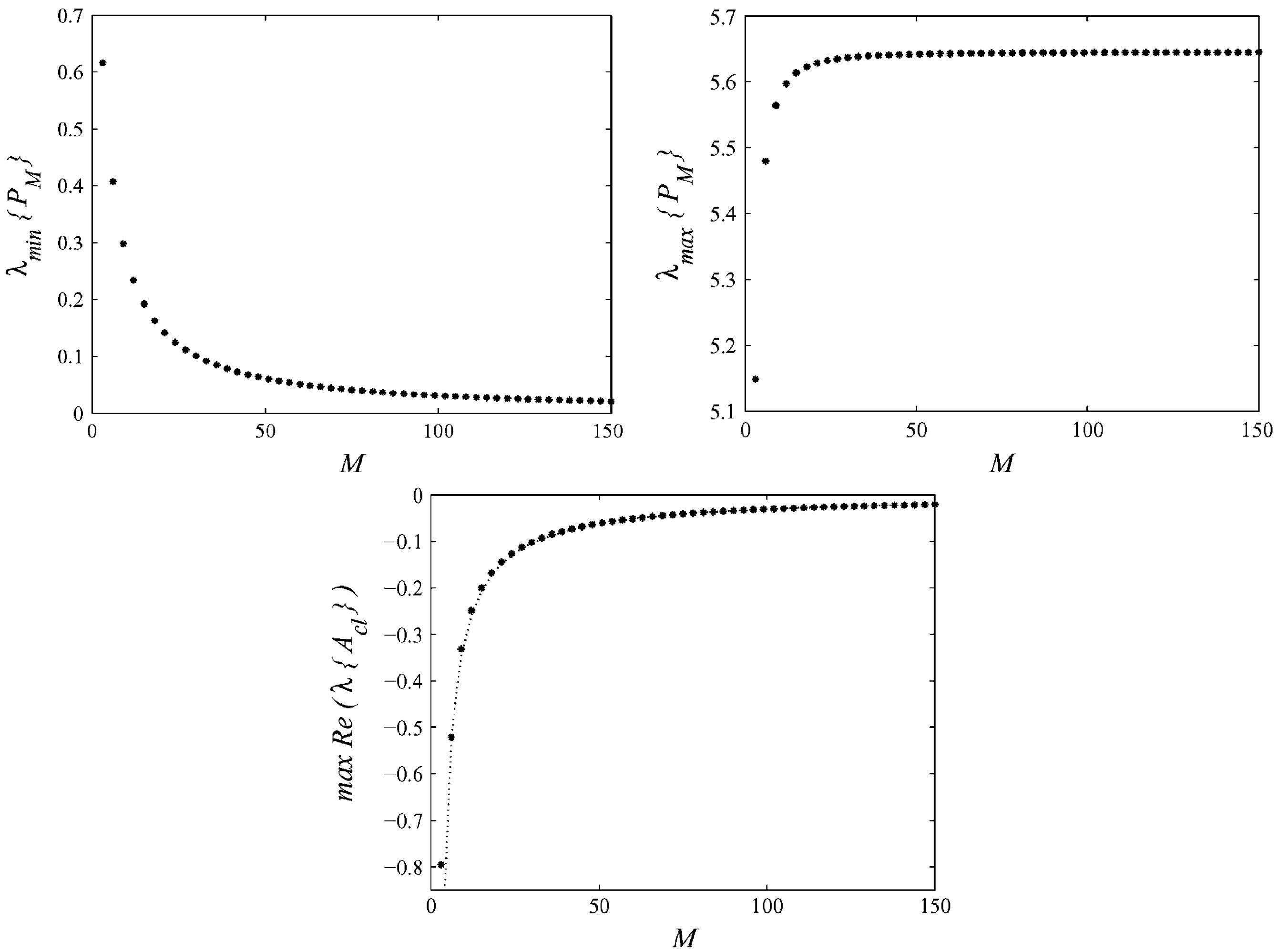

Fig. 3. Minimal (top left plot) and maximal eigenvalues (top right plot) of the ARE solution P_M for system (2) with performance index (5), and the dominant poles of LQR controlled platoon (2), (5) (bottom plot) as functions of the number of vehicles for $\{\kappa = 0, q_1 = q_3 = r = 1\}$.

inversely proportional manner to the number of vehicles in platoon. Hence, the time constant of the closed-loop system gets larger as the size of platoon increases. This is further demonstrated in Fig. 4, where the absolute and the relative position errors of an LQR controlled string (2), (5) with 20 and 50 vehicles are shown. Simulation results are obtained for $\{\xi_n(0) = \zeta_n(0) = 1, \forall n = \{1, \ldots, M\}\}$. These plots clearly exhibit the platoon size dependent rate of convergence toward the desired formation when a controller resulting from the LQR problem formulated by [2], [4] is implemented.

We remark that a formulation of the LQR problem for finite platoon (2) without the follow fictitious vehicle and appropriately modified cost functional of the form

$$J := \frac{1}{2}\int_0^\infty \left(\sum_{n=1}^{M} q_1\eta_n^2(t) + q_3\zeta_n^2(t) + r\tilde{u}_n^2(t)\right) \mathrm{d}t \qquad (7)$$

yields qualitatively similar results to the ones presented above (as can be seen from the top right plot of Fig. 5). On the other hand, for system (2) without both lead and follow fictitious vehicles, the appropriately modified performance index is given by (6). In this case, both the first and the last elements on the main diagonal of matrix Q_1 are equal to q_1. Based on the bottom plot of Fig. 5, it follows that the pair (Q, A) for system (2), (6) is practically not detectable, irrespective of the number of vehicles in formation. These numerical observations are confirmed analytically in Section II-C.

2) Levine and Athans [1]: The top left and top right plots in Fig. 6 respectively show minimal and maximal eigenvalues of the solution to the ARE in LQR problem (3), (6) with $\kappa = q_1 = q_3 = r = 1$. The bottom plot in the same figure shows the real parts of the least-stable poles of system (3) with a controller that minimizes (6). Clearly, $\lambda_{\max}\{P_M\}$ scales linearly with the number of vehicles and, thus, the optimal value of performance index (6) gets larger as the size of a vehicular string grows. This is because the pair $(\bar{A}, \bar{B})$ gets closer to losing its stabilizability when the platoon size increases. Equivalently, this can be established by observing the monotonic decay toward zero (with M) of the minimal singular value of $[\bar{A} - \lambda I\ \bar{B}]$ at $\lambda = 0$. In the interest of brevity, we do not show this dependence here. Furthermore, in the bottom plot, the dotted line represents the function $-2.222/M$, which implies the inversely proportional relationship between the dominant eigenvalues of the closed-loop A-matrix and the number of vehicles in platoon. This implies again that as the number of vehicles increases, there is no uniform bound on the decay rates of regulated states to zero. This is additionally illustrated in Fig. 7 where the relative position

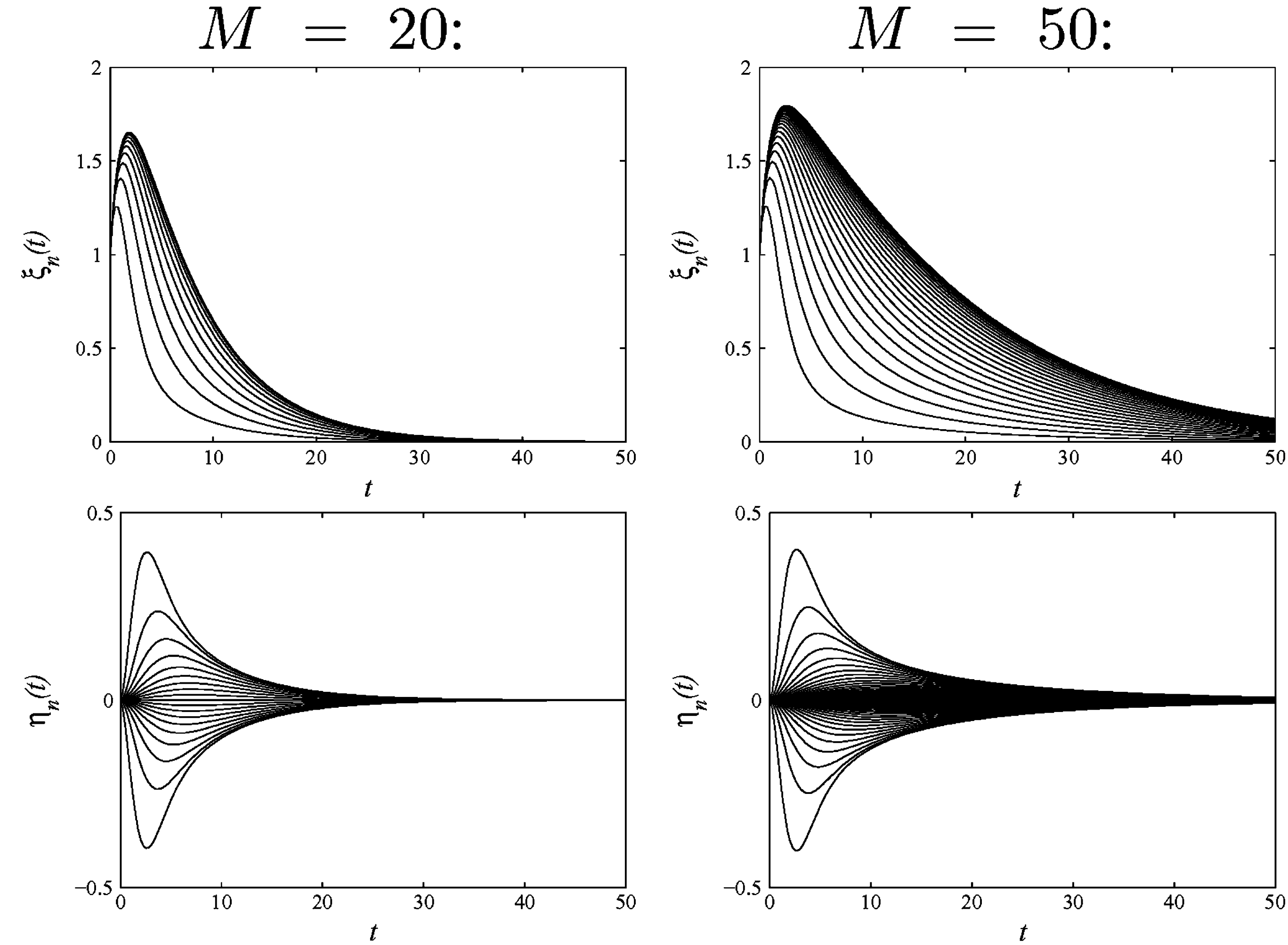

Fig. 4. Absolute and relative position errors of an LQR controlled string (2), (5) with 20 vehicles (left column) and 50 vehicles (right column), for $\{\kappa = 0, q_1 = q_3 = r = 1\}$. Simulation results are obtained for the following initial condition: $\{\xi_n(0) = \zeta_n(0) = 1, \forall\, n = \{1, \ldots, M\}\}$.

errors of an LQR controlled system (3), (6) with 20 and 50 vehicles are shown. Simulation results are obtained for $\{\eta_n(0) = 1, \forall\, n = \{2, \ldots, M\}; \zeta_n(0) = 1, \forall\, n = \{1, \ldots, M\}\}$.

The numerical computations of this section are strengthened by a rigorous analysis of finite platoons presented in Section II-C.

C. Analytical Results

In this section, we show that the LQR formulations of Melzer and Kuo [4] and Levine and Athans [1] are amenable to a thorough analysis which clarifies the numerical observations presented in Section II-B. Without loss of generality, we perform this analysis for a platoon in which every vehicle is modeled as a double integrator, that is $\ddot{x}_n = u_n$. In other words, we neglect the linearized drag coefficient per unit mass in (1).

1) Melzer and Kuo [4]: We recall that a state–space representation and the LQR weights in the formulation of Melzer and Kuo [4] with $\kappa = 0$ are

$$A = \begin{bmatrix} 0 & I \\ 0 & 0 \end{bmatrix} \quad B = \begin{bmatrix} 0 \\ I \end{bmatrix}$$
$$Q = \begin{bmatrix} q_1 T_M & 0 \\ 0 & q_3 I \end{bmatrix} \quad R = rI.$$

The corresponding LQR ARE for the components of matrix P

$$P := \begin{bmatrix} P_1 & P_0^* \\ P_0 & P_2 \end{bmatrix}$$

can then be decomposed into

$$P_0^* P_0 = r q_1 T_M \tag{8a}$$
$$P_2 P_2 = r(P_0 + P_0^* + q_3 I) \tag{8b}$$
$$P_1 = (1/r) P_2 P_0 = (1/r) P_0^* P_2. \tag{8c}$$

Represent P_0 as the sum of its symmetric and antisymmetric parts: $P_0 = P_{0s} + P_{0a}$. From (8b), it follows that P_{0s} commutes with P_2. Using this and (8c) we obtain the following Sylvester equation for P_{0a}:

$$(-P_2)P_{0a} + P_{0a}(-P_2) = 0.$$

Since $-P_2$ is a Hurwitz matrix, this equation has a unique solution $P_{0a} = 0$. Thus, $P_0 = P_0^*$, which renders (8) into

$$P_0 P_0 = r q_1 T_M$$
$$P_2 P_2 = r(2P_0 + q_3 I)$$
$$P_1 = (1/r) P_0 P_2.$$

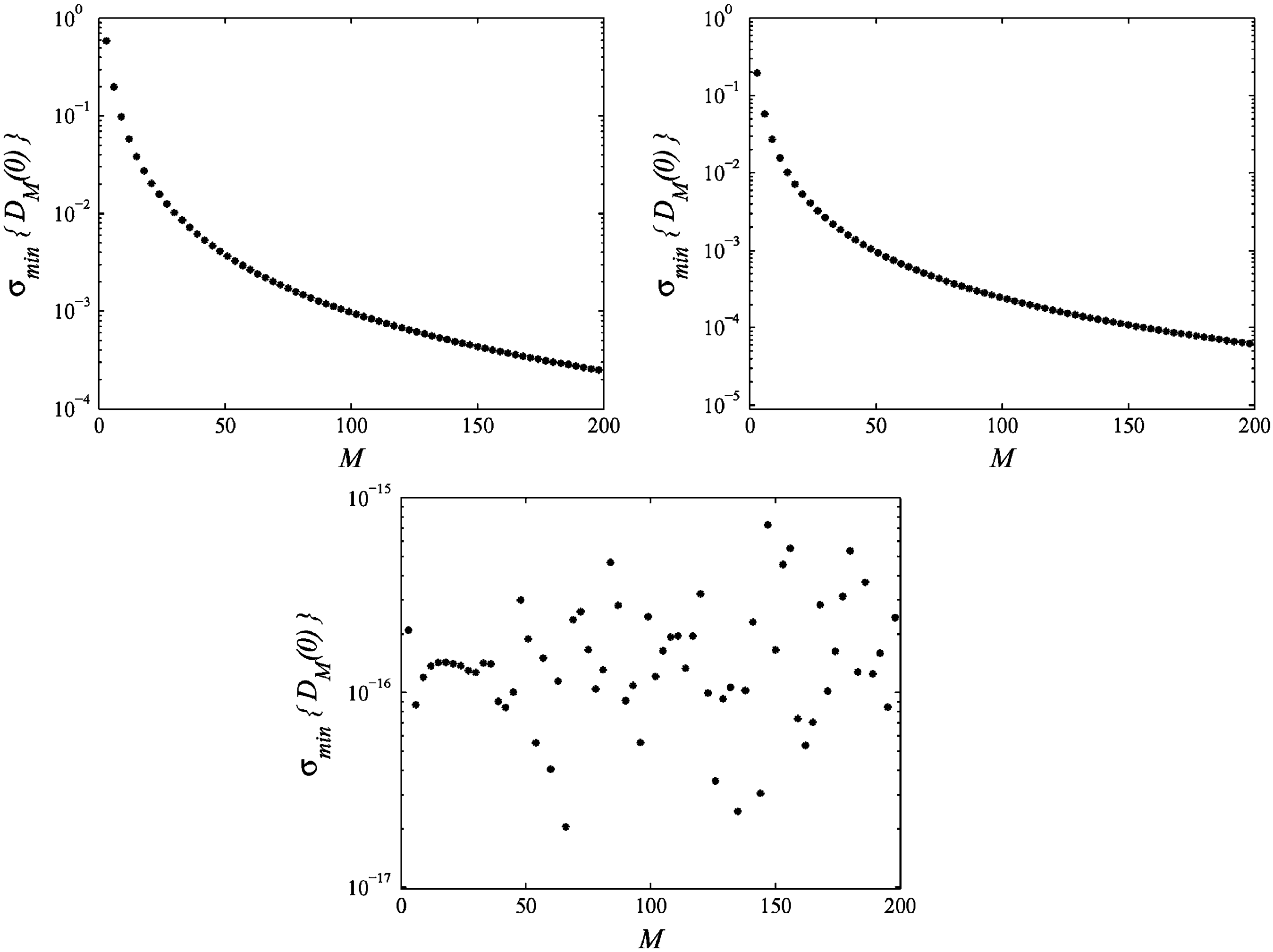

Fig. 5. Minimal singular values of matrix $D_M(\lambda) := [A^T - \lambda I \;\; Q^T]^T$ at $\lambda = 0$ for system (2) with performance objectives: (5) (top left plot), (7) (top right plot), and (6) (bottom plot) as functions of the number of vehicles for $\{\kappa = 0, q_1 = q_3 = r = 1\}$. These singular values are given in the logarithmic scale.

Hence, the unique positive–definite solution of the ARE is determined by

$$\begin{aligned} P_0 &= P_0^* = \sqrt{rq_1}\, T_M^{1/2} \\ P_2 &= \sqrt{r}\left(2\sqrt{rq_1}T_M^{1/2} + q_3 I\right)^{1/2} \\ P_1 &= \sqrt{q_1}\, T_M^{1/2}\left(2\sqrt{rq_1}T_M^{1/2} + q_3 I\right)^{1/2}. \end{aligned}$$

By performing a spectral decomposition of T_M

$$\begin{aligned} T_M = U\Lambda_T U^* \quad UU^* = U^*U = I \\ \Lambda_T = \mathrm{diag}\{\lambda_1(T_M), \ldots, \lambda_M(T_M)\} \end{aligned}$$

we can represent P_0, P_2, and P_1 as

$$P_0 = U\Lambda_0 U^* \quad P_2 = U\Lambda_2 U^* \quad P_1 = U\Lambda_1 U^*$$

where

$$\begin{aligned} \Lambda_0 &= \sqrt{rq_1}\, \Lambda_T^{1/2} \\ \Lambda_2 &= \sqrt{r}\left(2\sqrt{rq_1}\Lambda_T^{1/2} + q_3 I\right)^{1/2} \\ \Lambda_1 &= \sqrt{q_1}\, \Lambda_T^{1/2}\left(2\sqrt{rq_1}\Lambda_T^{1/2} + q_3 I\right)^{1/2}. \end{aligned}$$

It is noteworthy that the eigenvalues of T_M can be determined explicitly (see, for example, [5])

$$\lambda_n(T_M) = 2\left(1 - \cos\frac{n\pi}{M+1}\right), \qquad n \in \{1, \ldots, M\}. \tag{10}$$

The closed-loop A-matrix is given by

$$A_{\mathrm{cl}} = \begin{bmatrix} 0 & I \\ -(1/r)U\Lambda_0 U^* & -(1/r)U\Lambda_2 U^* \end{bmatrix}$$

which yields

$$\det(sI - A_{\mathrm{cl}}) = \det(s^2 I + (1/r)\Lambda_2\, s + (1/r)\Lambda_0).$$

Thus, the eigenvalues of A_{cl} are determined by the solutions to the following system of the uncoupled quadratic equations:

$$\begin{aligned} s_n^2 + b_n s_n + c_n = 0 \quad n \in \{1, \ldots, M\} \\ c_n := (\lambda_n(T_M) q_1/r)^{1/2} \\ b_n := (2c_n + q_3/r)^{1/2}. \end{aligned} \tag{11}$$

The distribution of the eigenvalues of the closed-loop A-matrix in an LQR controlled string (2), (5) of $M = 50$ vehicles with $\{\kappa = 0, q_1 = q_3 = r = 1\}$ is illustrated in Fig. 8.

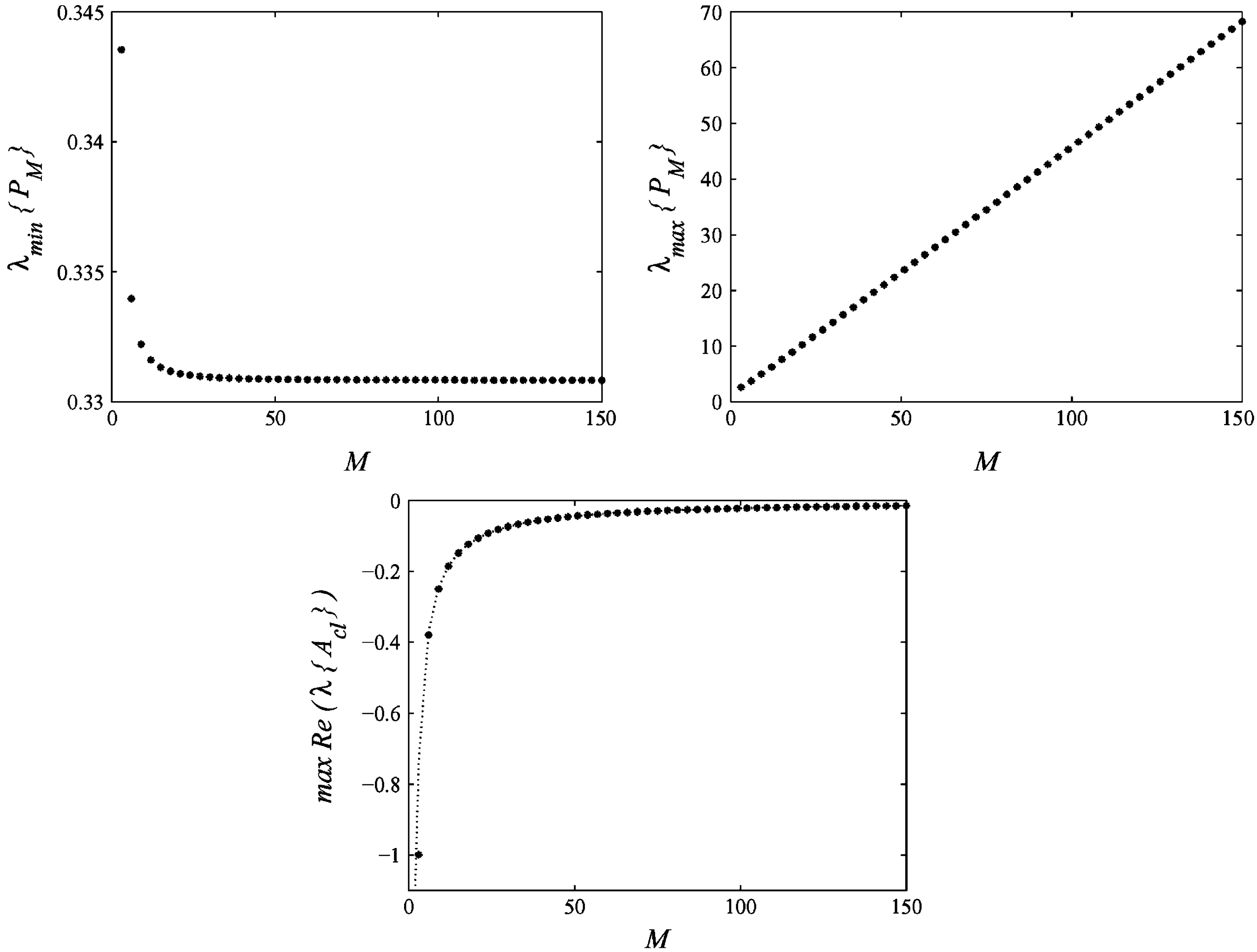

Fig. 6. Minimal (top left plot) and maximal eigenvalues (top right plot) of the ARE solution P_M for system (3) with performance index (6), and the dominant poles of LQR controlled platoon (3), (6) (bottom plot) as functions of the number of vehicles for $\kappa = q_1 = q_3 = r = 1$.

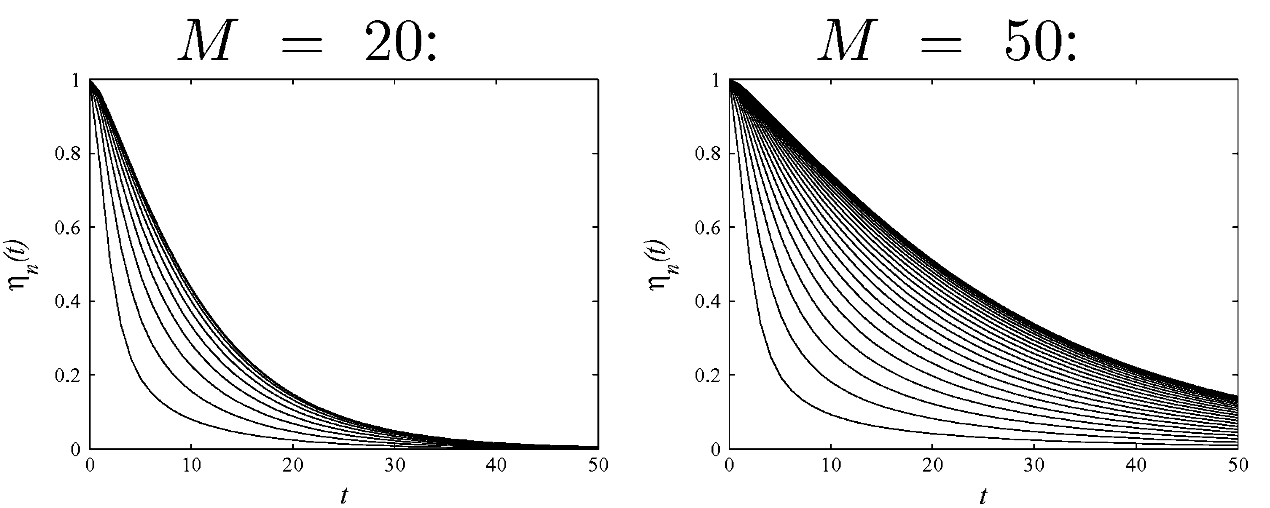

Fig. 7. Relative position errors of LQR controlled system (3), (6) with 20 vehicles (left plot) and 50 vehicles (right plot), for $\kappa = q_1 = q_3 = r = 1$. Simulation results are obtained for the following initial condition: $\{\eta_n(0) = 1, \forall\, n = \{2, \ldots, M\}; \zeta_n(0) = 1, \forall\, n = \{1, \ldots, M\}\}$.

We observe that

$$c_1^2 = 2(q_1/r)\left(1 - \cos\frac{\pi}{M+1}\right)$$

is a monotonically decaying function of the number of vehicles. Since c_1 converges to zero as M goes to infinity, there is an eigenvalue of A_{cl} that approaches imaginary axis in the limit of an infinite number of vehicles. As can be

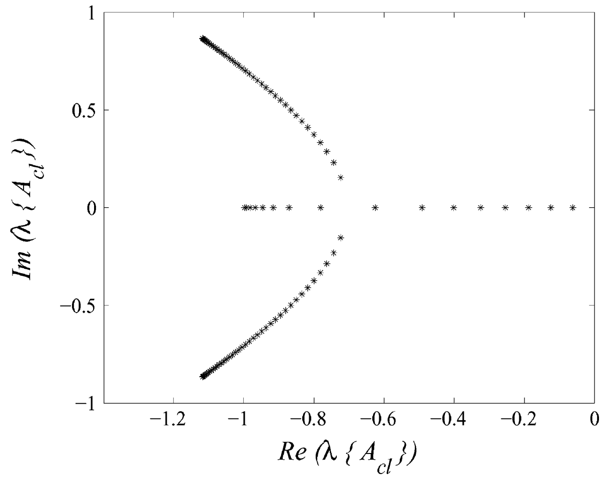

Fig. 8. Eigenvalues of the closed-loop A-matrix in an LQR controlled string (2), (5) of $M = 50$ vehicles with $\{\kappa = 0, q_1 = q_3 = r = 1\}$.

seen from the PBH detectability test, this is because the pair (Q, A) gets closer to loosing its detectability as the number of vehicles increases. Namely, since the singular values of $D_M(\lambda) := [A^T - \lambda I \;\; Q^T]^T$ at $\lambda = 0$ are determined by

$$\sigma_n(D_M(0)) = \begin{cases} q_1 \lambda_n(T_M), & n \in \{1, \ldots, M\} \\ q_3, & n \in \{M+1, \ldots, 2M\} \end{cases}$$

it follows from (10) that detectability of the pair (Q, A) degrades with the number of vehicles.

Furthermore, the eigenvalues of matrix P are given by the solutions to

$$s_n^2 + b_n\, s_n + c_n = 0, \qquad n \in \{1, \ldots, M\}$$

where

$$\begin{aligned} b_n &:= -\lambda_{2n}(\lambda_{0n}/r + 1) \\ &= -\sqrt{2\sqrt{r q_1 \lambda_n(T_M)} + q_3}\,(\sqrt{q_1 \lambda_n(T_M)} + \sqrt{r}) \\ c_n &:= \lambda_{0n}(\lambda_{0n} + q_3) \\ &= \sqrt{r q_1 \lambda_n(T_M)}(\sqrt{r q_1 \lambda_n(T_M)} + q_3). \end{aligned}$$

Clearly, c_n decays monotonically with M, which is in agreement with our numerical observations shown in the top left plot of Fig. 3.

2) Levine and Athans [1]: The LQR problem in the formulation of Levine and Athans [1] with $\kappa = 0$ is specified by

$$A = \begin{bmatrix} 0 & A_{12} \\ 0 & 0 \end{bmatrix} \quad B = \begin{bmatrix} 0 \\ I \end{bmatrix}$$
$$Q = \begin{bmatrix} q_1 I & 0 \\ 0 & q_3 I \end{bmatrix} \quad R = rI$$

where A_{12} represents an $(M-1) \times M$ Toeplitz matrix with the elements on the main diagonal and the first upper diagonal equal to -1 and 1, respectively. The LQR ARE for the components of matrix P

$$P := \begin{bmatrix} P_1 & P_0^* \\ P_0 & P_2 \end{bmatrix}$$

can be represented as

$$P_0^* P_0 = r q_1 I \tag{12a}$$
$$P_2 P_2 = r(P_0 A_{12} + A_{12}^* P_0^* + q_3 I) \tag{12b}$$
$$P_1 A_{12} = (1/r) P_0^* P_2 \tag{12c}$$
$$A_{12}^* P_1 = (1/r) P_2 P_0. \tag{12d}$$

By introducing the following notation:

$$V := P_0 A_{12} \quad L := A_{12}^* A_{12}$$

we rewrite (12) as

$$V^* V = r q_1 L \tag{13a}$$
$$P_2 P_2 = r(V + V^* + q_3 I) \tag{13b}$$
$$A_{12}^* P_1 A_{12} = (1/r) V^* P_2 = (1/r) P_2 V. \tag{13c}$$

Decompose V into the sum of its symmetric and antisymmetric parts: $V = V_s + V_a$. From (13b), it follows that V_s commutes with P_2. Using this and (13c), we obtain the following Sylvester equation for V_a:

$$(-P_2) V_a + V_a (-P_2) = 0.$$

Since $-P_2$ is a Hurwitz matrix, this equation has a unique solution $V_a = 0$. Thus, $V = V^*$, and (13) simplifies to

$$\begin{aligned} VV &= r q_1 L \\ P_2 P_2 &= r(2V + q_3 I) \\ A_{12}^* P_1 A_{12} &= (1/r) V P_2 = (1/r) P_2 V. \end{aligned}$$

Thus, the unique positive–definite solution of the ARE is determined by

$$\begin{aligned} V &= V^* = \sqrt{r q_1}\, L^{1/2} \\ P_2 &= \sqrt{r}\,(2\sqrt{r q_1}\, L^{1/2} + q_3 I)^{1/2}. \end{aligned}$$

By performing a spectral decomposition of L

$$L = U \Lambda_L U^* \quad U U^* = U^* U = I$$
$$\Lambda_L = \operatorname{diag}\{\lambda_1(L), \ldots, \lambda_M(L)\}$$

we can represent V and P_2 as

$$V = U \Lambda_V U^* \quad P_2 = U \Lambda_2 U^*$$

where

$$\Lambda_V = \sqrt{r q_1}\, \Lambda_L^{1/2} \quad \Lambda_2 = \sqrt{r}\, \left(2\sqrt{r q_1} \Lambda_L^{1/2} + q_3 I\right)^{1/2}.$$

Note that the nonzero eigenvalues of $L := A_{12}^* A_{12} \in \mathbb{R}^{M \times M}$ are equal to the eigenvalues of $T_{M-1} := A_{12} A_{12}^* \in \mathbb{R}^{(M-1)\times(M-1)}$, where T_{M-1} represents a symmetric Toeplitz matrix with the first row given by $[2\ -1\ 0 \cdots 0] \in \mathbb{R}^{M-1}$. These eigenvalues are determined by (see, for example, [5])

$$\lambda_n(T_{M-1}) = 2\left(1 - \cos\frac{n\pi}{M}\right), \qquad n \in \{1, \ldots, M-1\} \tag{15}$$

which gives

$$\lambda_n(L) = \begin{cases} \lambda_n(T_{M-1}) & n \in \{1, \ldots, M-1\} \\ 0 & n = M. \end{cases}$$

The closed-loop A-matrix is given by

$$A_{\text{cl}} = \begin{bmatrix} 0 & A_{12} \\ -(1/r) P_0 & -(1/r) P_2 \end{bmatrix}$$

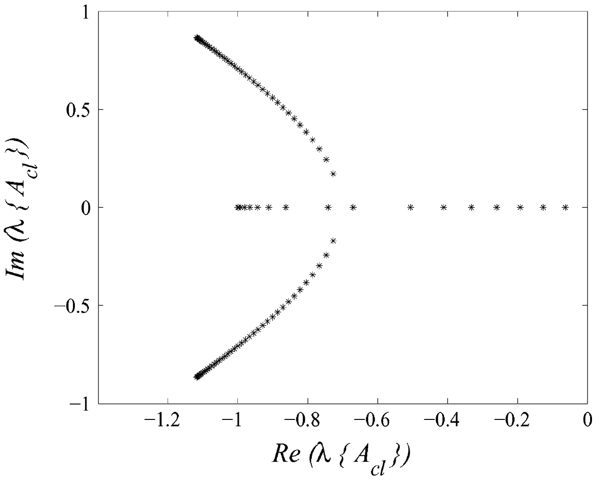

Fig. 9. Eigenvalues of the closed-loop A-matrix in an LQR controlled string (3), (6) of $M = 50$ vehicles with $\{\kappa = 0, q_1 = q_3 = r = 1\}$.

which yields

$$\det(sI - A_{\text{cl}}) = \frac{1}{s}\det(s^2 I + (1/r)P_2\, s + (1/r)V).$$

Based on this and the properties of matrix Λ_L, we conclude that A_{cl} has an eigenvalue at $-(q_3/r)^{1/2}$. The remaining eigenvalues of A_{cl} are determined by the solutions to the following system of the uncoupled quadratic equations:

$$\begin{aligned} s_n^2 + b_n s_n + c_n = 0 \quad n \in \{1, \ldots, M-1\} \\ c_n := (\lambda_n(T_{M-1})q_1/r)^{1/2} \\ b_n := (2c_n + q_3/r)^{1/2}. \end{aligned} \tag{16}$$

The eigenvalues of A_{cl} in an LQR controlled string (3), (6) of $M = 50$ vehicles with $\{\kappa = 0, q_1 = q_3 = r = 1\}$ are shown in Fig. 9.

Using similar argument as in Section II-C.1 we conclude that the closed-loop time constant increases as the number of vehicles gets larger. This is because stabilizability of the pair (A, B) degrades with the number of vehicles. Namely, based on (15) and the fact that the singular values of $S_M(\lambda) := [A - \lambda I\ B]$ at $\lambda = 0$ are given by

$$\sigma_n(S_M(0)) = \begin{cases} \lambda_n(T_{M-1}), & n \in \{1, \ldots, M-1\} \\ 1, & n \in \{M, \ldots, 2M-1\} \end{cases}$$

we conclude that the pair (A, B) gets closer to losing its stabilizability when the platoon size increases.

The results of this section clearly indicate that control strategies of [1], [2], and [4] lead to closed-loop systems with arbitrarily slow decay rates as the number of vehicles increases. In Section III, we show that the absence of a uniform rate of convergence in finite platoons manifests itself as the absence of exponential stability in the limit of an infinite vehicular strings.

III. Optimal Control of Infinite Platoons

In this section, we consider the LQR problem for infinite vehicular platoons. This problem was originally studied by Melzer and Kuo [2]. Using recently developed theory for spatially invariant linear systems [3], we show that the controller obtained by these authors does not provide exponential stability of the closed-loop system due to the lack of detectability of the pair (Q, A) in their LQR problem. We further demonstrate that the infinite platoon size limit of the problem formulation of Levine and Athans [1] yields an infinite-dimensional system which is not stabilizable.

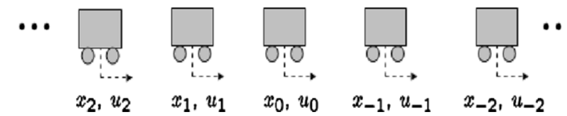

Fig. 10. Infinite platoon of vehicles.

A. Problem Formulation

A system of identical unit mass vehicles in an infinite string is shown in Fig. 10. The infinite-dimensional equivalents of (2) and (3) are, respectively, given by

$$\begin{aligned} \begin{bmatrix} \dot{\xi}_n \\ \dot{\zeta}_n \end{bmatrix} &= \begin{bmatrix} 0 & 1 \\ 0 & -\kappa \end{bmatrix} \begin{bmatrix} \xi_n \\ \zeta_n \end{bmatrix} + \begin{bmatrix} 0 \\ 1 \end{bmatrix} \tilde{u}_n \\ &=: A_n \psi_n + B_n \tilde{u}_n \quad n \in \mathbb{Z} \end{aligned} \tag{17}$$

and

$$\begin{aligned} \begin{bmatrix} \dot{\eta}_n \\ \dot{\zeta}_n \end{bmatrix} &= \begin{bmatrix} 0 & 1 - T_{-1} \\ 0 & -\kappa \end{bmatrix} \begin{bmatrix} \eta_n \\ \zeta_n \end{bmatrix} + \begin{bmatrix} 0 \\ 1 \end{bmatrix} \tilde{u}_n \\ &=: \bar{A}_n \phi_n + \bar{B}_n \tilde{u}_n, \qquad n \in \mathbb{Z} \end{aligned} \tag{18}$$

where T_{-1} is the operator of translation by -1 (in the vehicle's index). As in [2] and [6], we consider a quadratic cost functional of the form

$$J := \frac{1}{2}\int_0^\infty \sum_{n \in \mathbb{Z}} \left(q_1 \eta_n^2(t) + q_3 \zeta_n^2(t) + r\tilde{u}_n^2(t)\right) \mathrm{d}t \tag{19}$$

with q_1, q_3, and r being positive design parameters.

We utilize the fact that systems (17) and (18) have spatially invariant dynamics over a discrete spatial lattice $\mathbb{Z}$ [3]. This implies that the appropriate Fourier transform (in this case the bilateral Z-transform evaluated on the unit circle) can be used to convert analysis and quadratic design problems into those for a parameterized family of finite-dimensional systems. This transform, which we refer to here as the Z_θ-transform, is defined by

$$\hat{x}_\theta := \sum_{n \in \mathbb{Z}} x_n \mathrm{e}^{-jn\theta}.$$

Using this, system (17) and cost functional (19), respectively, transform to

$$\begin{aligned} \begin{bmatrix} \dot{\hat{\xi}}_\theta \\ \dot{\hat{\zeta}}_\theta \end{bmatrix} &= \begin{bmatrix} 0 & 1 \\ 0 & -\kappa \end{bmatrix} \begin{bmatrix} \hat{\xi}_\theta \\ \hat{\zeta}_\theta \end{bmatrix} + \begin{bmatrix} 0 \\ 1 \end{bmatrix} \hat{\tilde{u}}_\theta \\ &=: \hat{A}_\theta \hat{\psi}_\theta + \hat{B}_\theta \hat{\tilde{u}}_\theta \quad 0 \le \theta < 2\pi \\ J &= \frac{1}{4\pi}\int_0^\infty \int_0^{2\pi} (\hat{\psi}_\theta^*(t)\hat{Q}_\theta \hat{\psi}_\theta(t) \\ &\quad + \hat{\tilde{u}}_\theta^*(t)\hat{R}_\theta \hat{\tilde{u}}_\theta(t))\, \mathrm{d}\theta\, \mathrm{d}t \end{aligned} \tag{20}$$

where $\hat{R}_\theta := r$, and

$$\hat{Q}_\theta := \begin{bmatrix} 2q_1(1-\cos\theta) & 0 \\ 0 & q_3 \end{bmatrix}, \qquad 0 \le \theta < 2\pi.$$

Similarly, system (18) and cost functional (19) transform to

$$\begin{aligned} \begin{bmatrix} \dot{\hat{\eta}}_\theta \\ \dot{\hat{\zeta}}_\theta \end{bmatrix} &= \begin{bmatrix} 0 & 1-\mathrm{e}^{-j\theta} \\ 0 & -\kappa \end{bmatrix} \begin{bmatrix} \hat{\eta}_\theta \\ \hat{\zeta}_\theta \end{bmatrix} + \begin{bmatrix} 0 \\ 1 \end{bmatrix} \hat{\tilde{u}}_\theta \\ &=: \hat{\tilde{A}}_\theta \hat{\phi}_\theta + \hat{\tilde{B}}_\theta \hat{\tilde{u}}_\theta, 0 \le \theta < 2\pi \\ J &= \frac{1}{4\pi} \int_0^\infty \int_0^{2\pi} (\hat{\phi}_\theta^*(t) \hat{\tilde{Q}}_\theta \hat{\phi}_\theta(t) \\ &\quad + \hat{\tilde{u}}_\theta^*(t) \hat{R}_\theta \hat{\tilde{u}}_\theta(t)) \,\mathrm{d}\theta \,\mathrm{d}t \end{aligned} \tag{21}$$

respectively, where

$$\hat{\tilde{Q}}_\theta := \begin{bmatrix} q_1 & 0 \\ 0 & q_3 \end{bmatrix} \quad \hat{R}_\theta := r, \qquad 0 \le \theta < 2\pi.$$

If $(\hat{A}_\theta, \hat{B}_\theta)$ is stabilizable and $(\hat{Q}_\theta, \hat{A}_\theta)$ is detectable for all $\theta \in [0, 2\pi)$, then the θ-parameterized ARE

$$\hat{A}_\theta^* \hat{P}_\theta + \hat{P}_\theta \hat{A}_\theta + \hat{Q}_\theta - \hat{P}_\theta \hat{B}_\theta \hat{R}_\theta^{-1} \hat{B}_\theta^* \hat{P}_\theta = 0$$

has a unique positive–definite solution for every $\theta \in [0, 2\pi)$. This positive definite matrix determines the optimal stabilizing feedback for system (20) for every $\theta \in [0, 2\pi)$

$$\hat{\tilde{u}}_\theta := \hat{K}_\theta \hat{\psi}_\theta = -\hat{R}_\theta^{-1} \hat{B}_\theta^* \hat{P}_\theta \hat{\psi}_\theta \quad 0 \le \theta < 2\pi.$$

If this is the case, then there exist an exponentially stabilizing feedback for system (17) that minimizes (19), [3]. This optimal stabilizing feedback for (17) is given by

$$\tilde{u}_n = \sum_{k \in \mathbb{Z}} K_{n-k} \psi_k \quad n \in \mathbb{Z}$$

where

$$K_n = \frac{1}{2\pi} \int_0^{2\pi} \hat{K}_\theta \mathrm{e}^{jn\theta} \mathrm{d}\theta, \qquad n \in \mathbb{Z}.$$

B. Melzer and Kuo

It is clear that the pair $(\hat{A}_\theta, \hat{B}_\theta)$ in (20) is controllable for every $\theta \in [0, 2\pi)$. On the other hand, the pair $(\hat{Q}_\theta, \hat{A}_\theta)$ is not detectable at $\theta = 0$. In particular, the solution to the ARE at $\theta = 0$ is given by

$$\hat{P}_0 := \begin{bmatrix} 0 & 0 \\ 0 & r(-\kappa + \gamma) \end{bmatrix}$$

which yields the following closed-loop A-matrix at $\theta = 0$:

$$\hat{A}_{\mathrm{cl}0} = \begin{bmatrix} 0 & 1 \\ 0 & -\gamma \end{bmatrix} \tag{22}$$

with $\gamma := (1/r)\sqrt{(\kappa r)^2 + r q_3}$. Therefore, matrix $\hat{A}_{\mathrm{cl}0}$ is not Hurwitz, which implies that the solution to the LQR problem does not provide an exponentially stabilizing feedback for the original system [3]. We remark that this fact has not been realized in [2] and [6]. The spectrum of the closed-loop generator for $\{\kappa = 0, q_1 = q_3 = r = 1\}$ is shown in Fig. 11 to illustrate the absence of exponential stability.

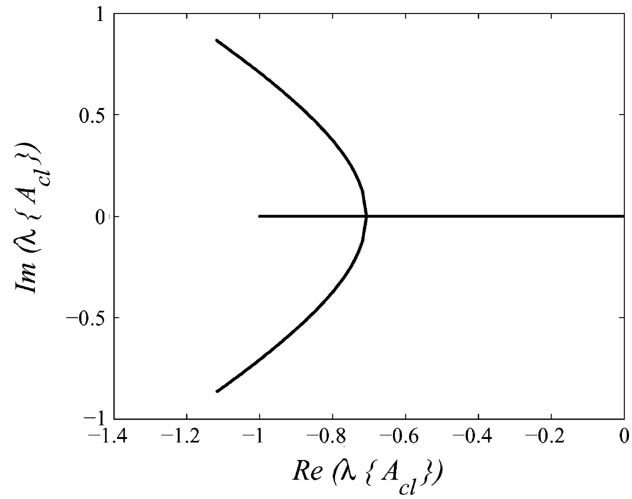

Fig. 11. Spectrum of the closed-loop generator in an LQR controlled spatially invariant string of vehicles (17) with performance index (19) and $\{\kappa = 0, q_1 = q_3 = r = 1\}$.

Remark 1: The spectrum of the closed-loop generator in an LQR controlled spatially invariant string of vehicles (17) with performance index (19) at $\kappa = 0$ is given by the solutions to the following θ-parameterized quadratic equation:

$$\begin{aligned} s_\theta^2 + b_\theta s_\theta + c_\theta = 0 \quad & \theta \in [0, 2\pi) \\ c_\theta &:= (2(q_1/r)(1 - \cos\theta))^{1/2} \\ b_\theta &:= (2c_\theta + q_3/r)^{1/2}. \end{aligned} \tag{23}$$

By comparing (10), (11), and (23), we see that the closed-loop eigenvalues of the finite platoon are points in the spectrum of the closed-loop infinite platoon. Furthermore, from these equations it follows that as the size of the finite platoon increases, this set of points becomes dense in the spectrum of the infinite platoon closed-loop A-operator. In this sense, the finite platoon is a convergent approximation to the infinite platoon, or alternatively, the infinite platoon is a useful paradigm for studying the large-scale, but finite platoon.

It is instructive to consider the initial states that are not stabilized by this LQR feedback. Based on (22), it follows that the solution of system (20) at $\theta = 0$ with the controller of [2] is determined by

$$\begin{aligned} \hat{\zeta}_0(t) &= \mathrm{e}^{-\gamma t} \hat{\zeta}_0(0) \\ \hat{\xi}_0(t) &= \hat{\xi}_0(0) - \frac{1}{\gamma}(1 - \mathrm{e}^{-\gamma t}) \hat{\zeta}_0(0). \end{aligned}$$

We have assumed that $\gamma \neq 0$, which can be accomplished for any $\kappa \ge 0$ by choosing $q_3 > 0$. Thus

$$\sum_{n \in \mathbb{Z}} \xi_n(t) = \sum_{n \in \mathbb{Z}} \xi_n(0) - \frac{1}{\gamma}(1 - \mathrm{e}^{-\gamma t}) \sum_{n \in \mathbb{Z}} \zeta_n(0)$$

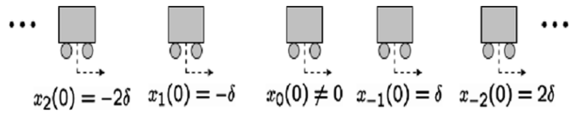

Fig. 12. Example of a position initial condition for which there is at least one vehicle whose absolute position error does not asymptotically converge to zero when the control strategy of [2] is used.

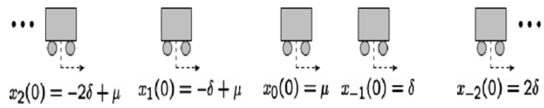

Fig. 13. Example of a position initial condition for which there is at least a pair of vehicles whose relative distance does not asymptotically converge to the desired intervehicular spacing δ when a control strategy of [1] is used.

which implies that $\lim_{t\to\infty}\sum_{n\in\mathbb{Z}}\xi_n(t) \neq 0$ unless

$$\sum_{n\in\mathbb{Z}}\xi_n(0) - \frac{1}{\gamma}\sum_{n\in\mathbb{Z}}\zeta_n(0) \equiv 0. \tag{24}$$

Therefore, if the initial condition of system (17) does not satisfy (24) than $\sum_{n\in\mathbb{Z}}\xi_n(t)$ cannot be asymptotically driven toward zero. It is not difficult to construct a physically relevant initial condition that violates (24). For example, this situation will be encountered if the string of vehicles at $t = 0$ cruises at the desired velocity v_d with all the vehicles being at their desired spatial locations except for a single vehicle. In other words, even for a seemingly benign initial condition of the form $\{\zeta_n(0) \equiv 0; \xi_n(0) = 0, \forall\, n \in \mathbb{Z}\setminus 0; \xi_0(0) = \mu \neq 0\}$ there exist at least one vehicle whose absolute position error does not converge to zero as time goes to infinity when the control strategy of Melzer and Kuo [2] is employed. This nonzero mean position initial condition is graphically illustrated in Fig. 12.

C. Levine and Athans

We note that system (21) is not stabilizable at $\theta = 0$, which prevents system (18) from being stabilizable [3]. Hence, when infinite vehicular platoons are considered the formulation of design problem of Levine and Athans [1] is ill-posed (that is, unstabilizable). In particular, the solution of the "$\hat{\eta}$-subsystem" of (21) at $\theta = 0$ does not change with time, that is $\hat{\eta}_0(t) \equiv \hat{\eta}_0(0)$, which indicates that $\sum_{n\in\mathbb{Z}}\eta_n(t) \equiv \sum_{n\in\mathbb{Z}}\eta_n(0)$. Therefore, for a nonzero mean initial condition $\{\eta_n(0)\}_{n\in\mathbb{Z}}$, the sum of all relative position errors is identically equal to a nonzero constant determined by $\sum_{n\in\mathbb{Z}}\eta_n(0)$. An example of such initial condition is given by $\{\eta_n(0) = 0, \forall\, n \in \mathbb{Z}\setminus 0; \eta_0(0) = \mu \neq 0\}$, and it is illustrated in Fig. 13. It is quite remarkable that the control strategy of Levine and Athans [1] is not able to asymptotically steer all relative position errors toward zero in an infinite platoon with this, at first glance, innocuously looking initial condition.

Therefore, we have shown that exponential stability of an LQR controlled infinite platoon cannot be achieved due to the lack of detectability (in the case of [2] and [4]) and stabilizability (in the case of [1]). These facts have very important practical implications for optimal control of large vehicular platoons. Namely, our analysis clarifies results of Section II, where we have observed that decay rates of a finite platoon with controllers of [1], [2], and [4] become smaller as the platoon size increases.

In Section IV, we demonstrate that exponential stability of an infinite string of vehicles can be guaranteed by accounting for position errors with respect to absolute desired trajectories in both the state–space representation and the performance criterion.

IV. Alternative Problem Formulations

In this section, we propose an alternative formulation of optimal control problems for vehicular platoons. In particular, we study distributed optimal control design with respect to quadratic performance criteria (LQR, $\mathcal{H}_2, \mathcal{H}_\infty$), and show that the problems discussed in Sections II and III can be overcome by accounting for the absolute position errors in both the state–space realization and the performance criterion. We also briefly remark on the choice of the appropriate state–space.

A. Alternative LQR Problem Formulation

In this section, we suggest an alternative formulation of the LQR problem in order to overcome issues raised in Section II and Section III. Since consideration of infinite platoons is better suited for analysis, we first study the LQR problem for a spatially invariant string of vehicles, and then discuss practical implications for optimal control of finite vehicular platoons.

We represent system shown in Fig. 10 by its state–space representation (17) expressed in terms of absolute position and velocity error variables, and propose the quadratic performance index

$$J = \frac{1}{2}\int_0^\infty \sum_{n\in\mathbb{Z}} \big(q_1\eta_n^2(t) + q_2\xi_n^2(t) + q_3\zeta_n^2(t) + r\tilde{u}_n^2(t)\big)\,\mathrm{d}t \tag{25}$$

with q_1, q_2, q_3, and r being positive design parameters. It should be noted that in (25) we account for both absolute position errors ξ_n and relative position errors η_n. This is in contrast to performance index (19) considered by Melzer and Kuo [2] and Chu [6], where only relative position errors are penalized in J. The main point of this section is to show that if one accounts for absolute position errors in the cost functional, then LQR feedback will be exponentially stabilizing.

Application of Z_θ-transform renders (17) into (20), whereas (25) simplifies to

$$J = \frac{1}{4\pi}\int_0^\infty\int_0^{2\pi} (\hat{\psi}_\theta^*(t)\hat{Q}_\theta^\star\hat{\psi}_\theta(t) + \hat{\tilde{u}}_\theta^*(t)\hat{R}_\theta\hat{\tilde{u}}_\theta(t))\,\mathrm{d}\theta\,\mathrm{d}t$$

where $\hat{R}_\theta := r$, and

$$\hat{Q}_\theta^\star := \begin{bmatrix} q_2 + 2q_1(1-\cos\,\theta) & 0 \\ 0 & q_3 \end{bmatrix}, \qquad 0 \le \theta < 2\pi.$$

As shown in Section III, the pair $(\hat{A}_\theta, \hat{B}_\theta)$ is controllable for every $\theta \in [0, 2\pi)$. Furthermore, it is easily established that the pair $(\hat{Q}_\theta^\star, \hat{A}_\theta)$ is detectable if and only if

$$q_2 + 2q_1(1-\cos\theta) \neq 0 \quad \forall\, \theta \in [0, 2\pi).$$

Even if q_1 is set to zero, this condition is satisfied as long as $q_2 > 0$. However, in this situation the intervehicular spacing is not penalized in the cost functional which may result into an unsafe control strategy. Because of that, as in [2] and [6], we assign

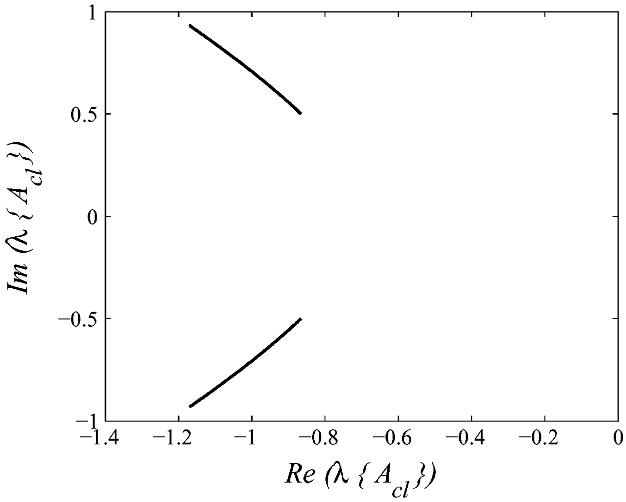

Fig. 14. Spectrum of the closed-loop generator in an LQR controlled spatially invariant string of vehicles (17) with performance index (25) and $\{\kappa = 0, q_1 = q_2 = q_3 = r = 1\}$.

a positive value to q_1. In this case, if $q_2 = 0$, the pair $(\hat{Q}^{\star}_{\theta}, \hat{A}_{\theta})$ is not detectable at $\theta = 0$, which implies that accounting for the absolute position errors in the performance criterion is essential for obtaining a stabilizing solution to the LQR problem. The spectrum of the closed-loop generator shown in Fig. 14 illustrates exponential stability of infinite string of vehicles (17) combined in feedback with a controller that minimizes performance index (25) for $\{\kappa = 0, q_1 = q_2 = q_3 = r = 1\}$.

For a finite platoon with M vehicles the appropriately modified version of (25) is obtained by adding an additional term that accounts for the absolute position errors to the right-hand side of (5)

$$J := \frac{1}{2}\int_0^{\infty} \sum_{n=1}^{M+1} q_1 \eta_n^2(t)\,\mathrm{d}t + \frac{1}{2}\int_0^{\infty} \sum_{n=1}^{M} \left(q_2 \xi_n^2(t) + q_3 \zeta_n^2(t) + r\tilde{u}_n^2(t)\right)\mathrm{d}t. \quad (26)$$

Equivalently, (26) can be rewritten as

$$J = \frac{1}{2}\int_0^{\infty} (\psi^*(t) Q^{\star} \psi(t) + \tilde{u}^*(t) R \tilde{u}(t))\,\mathrm{d}t$$

where $Q^{\star}$ and R are $2M \times 2M$ and $M \times M$ matrices given by

$$Q^{\star} := \begin{bmatrix} Q_1 + q_2 I & 0 \\ 0 & q_3 I \end{bmatrix} \quad R := rI$$

respectively. Toeplitz matrix Q_1 has the same meaning as in Section II.

The top left and top right plots in Fig. 15, respectively, show the minimal and maximal eigenvalues of the ARE solution for system (2) with performance index (26), and the right plot in the same figure shows the real parts of the least-stable poles in an LQR controlled string of vehicles (2), (26) for $\{\kappa = 0, q_1 = q_2 = q_3 = r = 1\}$. Clearly, when the absolute position errors are accounted for in both the state–space realization and J, the problems addressed in Section II are easily overcome. In particular, the least-stable closed-loop eigenvalues converge toward a nonzero value determined by the dominant pole of the spatially invariant system.

Absolute position errors of an LQR controlled string (2), (26) with 20 and 50 vehicles are shown in Fig. 16. Simulation results are obtained for $\{\kappa = 0, q_1 = q_2 = q_3 = r = 1\}$ and the initial condition of the form $\{\xi_n(0) = \zeta_n(0) = 1, \forall n = \{1, \ldots, M\}\}$. These plots clearly demonstrate the uniform rate of convergence toward the desired formation. This is accomplished by expressing the state–space realization in terms of the errors with respect to the absolute desired trajectories and by accounting for the absolute position errors in the performance index.

We note that qualitatively similar results are obtained if LQR problem is formulated for system (2) with either functional (7) or functional (6) augmented by a term penalizing absolute position errors.

In Section IV-B, we formulate the distributed $\mathcal{H}_2$ and $\mathcal{H}_\infty$ design problems for a spatially invariant string of vehicles, and discuss necessary conditions for the existence of stabilizing controllers.

B. $\mathcal{H}_2$ and $\mathcal{H}_\infty$ Control of Spatially Invariant Platoons

In this section, we consider a spatially invariant string of vehicles shown in Fig. 10 in the presence of external disturbances

$$\ddot{x}_n + \kappa \dot{x}_n = u_n + d_n, \qquad n \in \mathbb{Z} \quad (27)$$

and formulate $\mathcal{H}_2$ and $\mathcal{H}_\infty$ control problems. A disturbance acting on the nth vehicle is denoted by d_n and it can account for the external forces such as wind gusts, rolling resistance friction, pot holes, and nonhorizontal road slopes. For simplicity, we assume that there are no model uncertainties and rewrite (27) in the form suitable for solving a standard robust control problem [7]

$$\begin{aligned} \dot{\psi}_n &= A\psi_n + B_1 w_n + B_2 \tilde{u}_n \\ z_n &= C_1 \psi_n + D_{11} w_n + D_{12} \tilde{u}_n \\ y_n &= C_2 \psi_n + D_{21} w_n + D_{22} \tilde{u}_n \end{aligned} \quad (28)$$

for every $n \in \mathbb{Z}$, where

$$\psi_n := \begin{bmatrix} \xi_n \\ \zeta_n \end{bmatrix} \quad \tilde{u}_n := u_n - \kappa v_d \quad w_n := \begin{bmatrix} d_n \\ \nu_n \end{bmatrix}$$

with ν_n denoting the measurement noise for the nth vehicle. With these choices, matrices A, B_1, and B_2 are, respectively, determined by

$$A := \begin{bmatrix} 0 & 1 \\ 0 & -\kappa \end{bmatrix} \quad B_1 := \begin{bmatrix} 0 & 0 \\ 1 & 0 \end{bmatrix} \quad B_2 := \begin{bmatrix} 0 \\ 1 \end{bmatrix}.$$

We further assume the "exogenous" and "sensed" outputs for the nth vehicle of the form

$$z_n := \begin{bmatrix} q_1(\xi_n - \xi_{n-1}) \\ q_2 \xi_n \\ q_3 \zeta_n \\ r\tilde{u}_n \end{bmatrix} \quad y_n := \xi_n + s_1 \nu_n$$

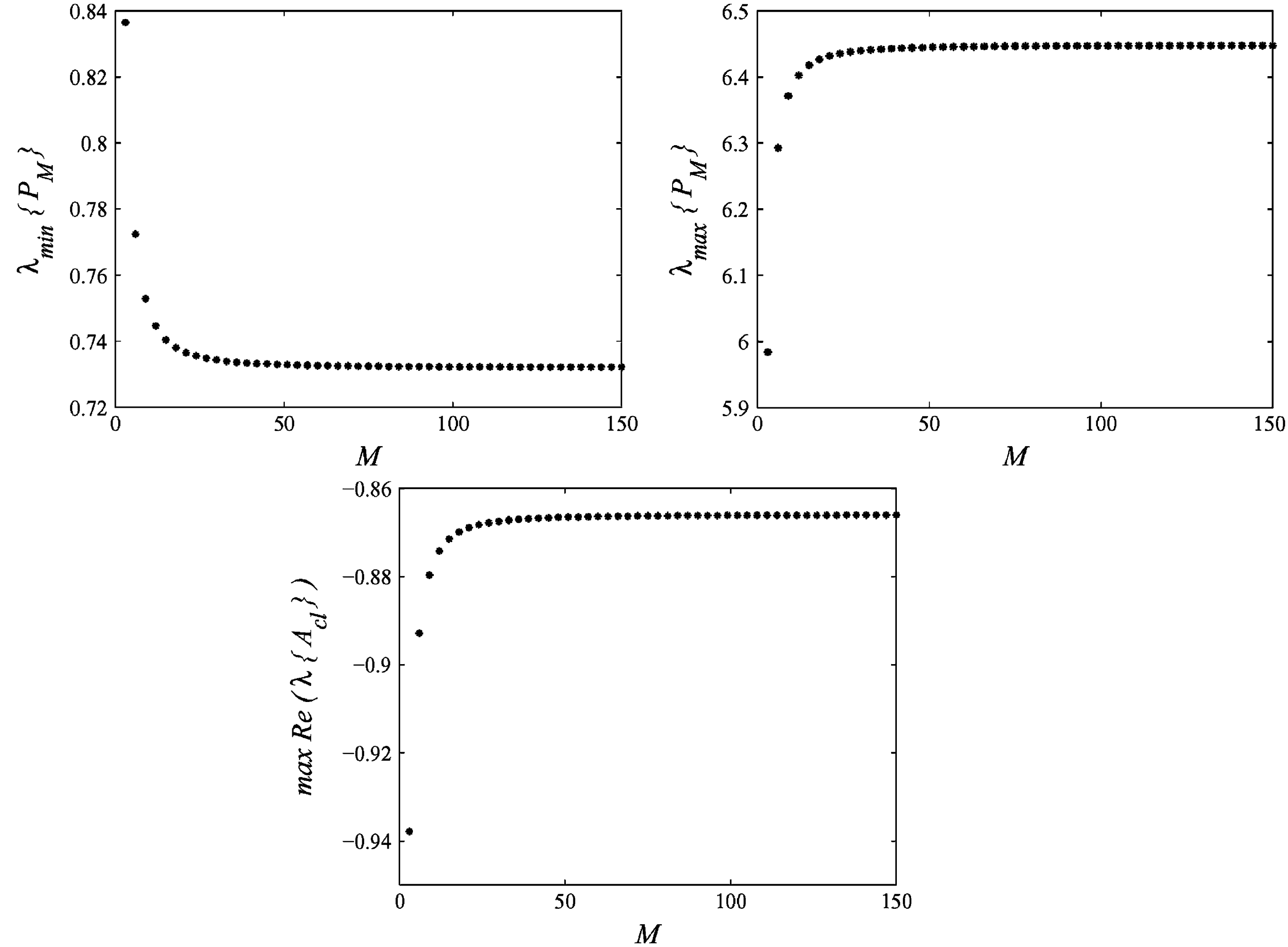

Fig. 15. Minimal (top left plot) and maximal eigenvalues (top right plot) of the ARE solution P_M for system (2) with performance index (26), and the dominant poles of LQR controlled platoon (2), (26) (bottom plot) as functions of the number of vehicles, for $\{\kappa = 0, q_1 = q_2 = q_3 = r = 1\}$.

where q_1, q_2, q_3, r, and s_1 represent positive design parameters. Thus, operators C_i and D_{ij}, for every $i, j = \{1, 2\}$, are determined by

$$C_1 := \begin{bmatrix} q_1(1 - T_{-1}) & 0 \\ q_2 & 0 \\ 0 & q_3 \\ 0 & 0 \end{bmatrix} \quad C_2 := [1\ 0]$$
$$D_{11} := 0 \quad D_{12} := [0\ 0\ 0\ r]^*$$
$$D_{21} := [0\ s_1] \quad D_{22} := 0.$$

Application of Z_θ-transform renders (28) into the θ-parameterized finite dimensional family of systems

$$\begin{aligned} \dot{\hat{\psi}}_\theta &= \hat{A}_\theta \hat{\psi}_\theta + \hat{B}_{1\theta} \hat{w}_\theta + \hat{B}_{2\theta} \hat{\tilde{u}}_\theta \\ \hat{z}_\theta &= \hat{C}_{1\theta} \hat{\psi}_\theta + \hat{D}_{11\theta} \hat{w}_\theta + \hat{D}_{12\theta} \hat{\tilde{u}}_\theta \\ \hat{y}_\theta &= \hat{C}_{2\theta} \hat{\psi}_\theta + \hat{D}_{21\theta} \hat{w}_\theta + \hat{D}_{22\theta} \hat{\tilde{u}}_\theta \end{aligned} \tag{29}$$

with $\theta \in [0, 2\pi)$, and

$$\hat{A}_\theta = \begin{bmatrix} 0 & 1 \\ 0 & -\kappa \end{bmatrix} \quad \hat{B}_{1\theta} = \begin{bmatrix} 0 & 0 \\ 1 & 0 \end{bmatrix}$$
$$\hat{B}_{2\theta} = \begin{bmatrix} 0 \\ 1 \end{bmatrix} \quad \hat{C}_{1\theta} = \begin{bmatrix} q_1(1 - \mathrm{e}^{-j\theta}) & 0 \\ q_2 & 0 \\ 0 & q_3 \\ 0 & 0 \end{bmatrix}$$
$$\hat{D}_{11\theta} = 0 \quad \hat{D}_{12\theta} = [0\ 0\ 0\ r]^*$$
$$\hat{C}_{2\theta} = [1\ 0] \quad \hat{D}_{21\theta} = [0\ s_1] \quad \hat{D}_{22\theta} = 0.$$

Solving the distributed $\mathcal{H}_2$ and $\mathcal{H}_\infty$ design problems for system (28) amounts to solving the $\mathcal{H}_2$ and $\mathcal{H}_\infty$ design problems for a parameterized family of finite-dimensional linear time-invariant (LTI) systems (29) over $\theta \in [0, 2\pi)$ [3].

The following properties of (29) are readily established.

1) Pairs $(\hat{A}_\theta, \hat{B}_{2\theta})$ and $(\hat{C}_{2\theta}, \hat{A}_\theta)$ are respectively stabilizable and detectable for every $\theta \in [0, 2\pi)$.
2) $\hat{D}^*_{12\theta} \hat{D}_{12\theta} = r^2 > 0, \forall \theta \in [0, 2\pi)$.
3) $\hat{D}_{21\theta} \hat{D}^*_{21\theta} = s_1^2 > 0, \forall \theta \in [0, 2\pi)$.
4) $\hat{D}^*_{12\theta} \hat{C}_{1\theta} = 0, \hat{B}_{1\theta} \hat{D}^*_{21\theta} = 0, \forall \theta \in [0, 2\pi)$.
5) Pair $(\hat{A}_\theta, \hat{B}_{1\theta})$ is stabilizable for every $\theta \in [0, 2\pi)$. Pair $(\hat{C}_{1\theta}, \hat{A}_\theta)$ is detectable for every $\theta \in [0, 2\pi)$ if and only if $q_2 \neq 0$.

If properties 4) and 5) hold, then

$$\sigma_{\min} \left\{ \begin{bmatrix} \hat{A}_\theta - j\omega I & \hat{B}_{2\theta} \\ \hat{C}_{1\theta} & \hat{D}_{12\theta} \end{bmatrix} \right\} \geq \varepsilon > 0 \tag{30a}$$
$$\sigma_{\min} \left\{ \begin{bmatrix} \hat{A}_\theta - j\omega I & \hat{B}_{1\theta} \\ \hat{C}_{2\theta} & \hat{D}_{21\theta} \end{bmatrix} \right\} \geq \varepsilon > 0 \tag{30b}$$

$\{\forall \theta \in [0, 2\pi), \forall \omega \in \mathbb{R}\}$ which are necessary conditions for the existence of exponentially stabilizing solutions to these infinite

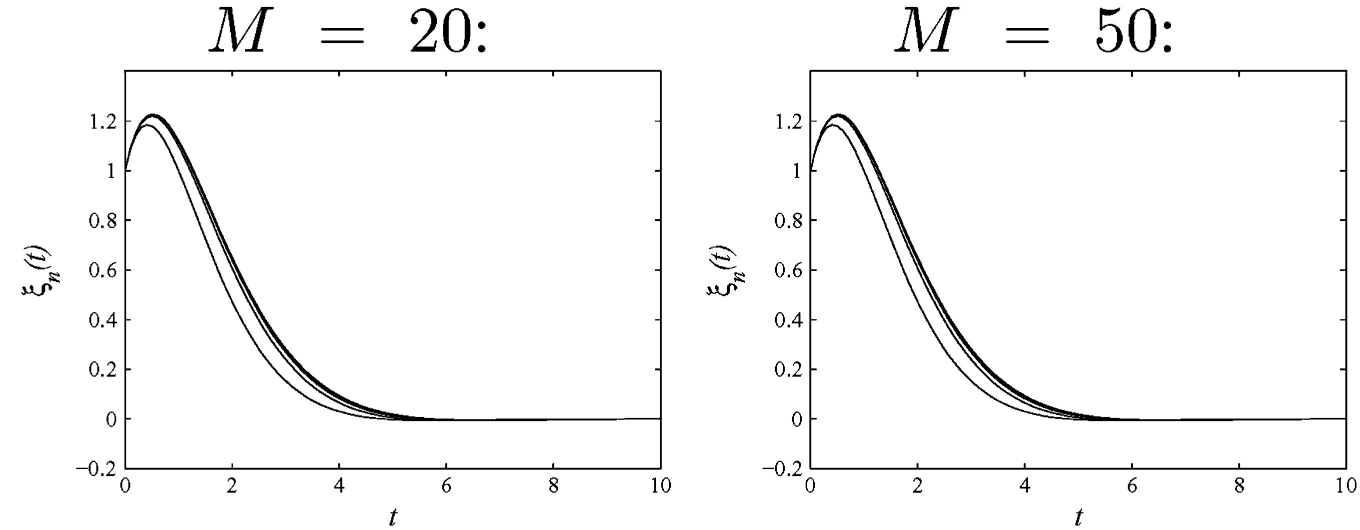

Fig. 16. Absolute position errors of an LQR controlled string (2), (26) with 20 vehicles (left plot) and 50 vehicles (right plot), for $\{\kappa = 0, q_1 = q_2 = q_3 = r = 1\}$. Simulation results are obtained for the following initial condition: $\{\xi_n(0) = \zeta_n(0) = 1, \forall\, n = \{1, \ldots, M\}\}$.

dimensional $\mathcal{H}_2$ and $\mathcal{H}_\infty$ control problems [3]. It is noteworthy that condition (30a) is going to be violated unless $q_2 \neq 0$. This further underlines the importance of incorporating the absolute position errors in the performance index.

In Section IV-C, we briefly comment on the initial conditions that cannot be dealt with the quadratically optimal controllers of this section.

C. On the Choice of the Appropriate State–Space

In this section, we remark on the initial conditions that are not square summable (in a space of the absolute errors) and as such are problematic for optimal controllers involving quadratic criteria.

Motivated by example shown in Fig. 13 we note that the initial relative position errors $\{\eta_n(0)\}_{n\in\mathbb{Z}}$ cannot be nonzero mean unless the absolute position errors at $t = 0$ sum to infinity. Namely, if $\sum_{n\in\mathbb{Z}} \xi_n(0)$ is bounded, then

$$\begin{aligned}\sum_{n\in\mathbb{Z}} \eta_n(0) &:= \sum_{n\in\mathbb{Z}} (\xi_n(0) - \xi_{n-1}(0)) \\ &= \sum_{n\in\mathbb{Z}} \xi_n(0) - \sum_{n\in\mathbb{Z}} \xi_{n-1}(0) = 0.\end{aligned}$$

Clearly, for the initial condition shown in Fig. 13, that is

$$\begin{aligned} x_n(0) &= -n\delta + \mu \quad \forall\, n \in \mathbb{N}_0 \\ x_n(0) &= -n\delta \qquad\;\; \forall\, n \in \mathbb{Z} \setminus \mathbb{N}_0\end{aligned}$$

sequence $\{\xi_n(0)\}_{n\in\mathbb{Z}}$ sums to infinity if $\mu \neq 0$. In addition to that, $\{\xi_n(0)\}_{n\in\mathbb{Z}} \notin l_2$, whereas $\{\eta_n(0)\}_{n\in\mathbb{Z}} \in l_2$. Therefore, despite the fact that the intervehicular spacing for all but a single vehicle is kept at the desired level δ, a relevant nonsquare summable initial condition (in a space of the absolute position errors) is easily constructed. It is worth noting that LQR, $\mathcal{H}_2$, and $\mathcal{H}_\infty$ controllers of Section IV are derived under the assumption of the square summable initial conditions and as such cannot be used for guarding against an entire class of physically relevant initial states. This illustrates that a Hilbert space l_2 may represent a rather restrictive choice for the underlying state–space of (17). Perhaps the more appropriate state–space for this system is a Banach space l_∞. The control design on this state–space is outside the scope of this work. We refer the reader to [8] for additional details.

V. LQR Design for a Platoon of Vehicles Arranged in a Circle

In this section, we consider the LQR problem for a platoon of M vehicles arranged in circle. This is an idealization of the case of equally spaced vehicles on a closed track. As we show, this problem is analytically solvable since it represents a spatially invariant system on the discretized circle. We use this solution to address the possibility of whether one can impose uniform rates of convergence in the formulation of Levine and Athans [1] by appropriate selection of weights. For a certain class of weights, we show that if one imposes a uniform bound on closed-loop time constants, then high-gain feedback results. Specifically, the feedback gains increase with the size of the platoon. This is a rather intuitive result and we obtain explicit bounds for this analytically solvable case.

The control objective is the same as before: to drive the entire platoon at the constant cruising velocity v_d, and to keep the distance between the neighboring vehicles at a prespecified constant level δ. Clearly, this is possible only if the radius of a circle is given by $r_M = M\delta/2\pi$. For simplicity, we neglect the linearized drag coefficient per unit mass in (1), and model each vehicle as a double integrator, that is $\ddot{x}_n = u_n$. Under this assumption, the state–space representation of Levine and Athans [1] is given by

$$\begin{aligned}\begin{bmatrix}\dot{\eta}_n \\ \dot{\zeta}_n\end{bmatrix} &= \begin{bmatrix} 0 & 1 - T_{-1} \\ 0 & 0\end{bmatrix}\begin{bmatrix}\eta_n \\ \zeta_n\end{bmatrix} + \begin{bmatrix}0 \\ 1\end{bmatrix} u_n \\ &=: A_n\phi_n + B_n u_n \end{aligned} \tag{31}$$

where $\xi_n(t) := x_n(t) - v_d t - n\delta, \eta_n(t) := \xi_n(t) - \xi_{n-1}(t), \zeta_n(t) := \dot{\xi}_n(t) = \dot{x}_n(t) - v_d$, and T_{-1} is the operator of translation by -1 (in the vehicle's index). Note that (31) is subject to the following constraint:

$$\sum_{n=0}^{M-1} \eta_n(t) = 0 \tag{32}$$

for every $t \geq 0$. This follows directly from the definition of the relative position errors and the fact that a circular vehicular platoon is considered.

We propose the following cost functional:

$$\begin{aligned} J := &\frac{1}{2}\int_0^\infty \sum_{n=0}^{M-1}\sum_{m=0}^{M-1} \eta_n^*(t) q_{p,n-m}\eta_m(t)\,\mathrm{d}t \\ &+ \frac{1}{2}\int_0^\infty \sum_{n=0}^{M-1}\sum_{m=0}^{M-1} \zeta_n^*(t) q_{v,n-m}\zeta_m(t)\,\mathrm{d}t \\ &+ \frac{1}{2}\int_0^\infty \sum_{n=0}^{M-1}\sum_{m=0}^{M-1} u_n^*(t) r_{n-m} u_m(t)\,\mathrm{d}t \end{aligned} \tag{33}$$

where all arithmetic with indices is done $(\mathrm{mod}\, M)$. This cost functional can be better understood as follows: If the sequences $\{\eta_m\}, \{\zeta_m\}$, and $\{u_m\}$ are arranged each in vectors denoted by η, ζ, and u, respectively, then J can be rewritten as

$$J = \frac{1}{2}\int_0^\infty (\eta^* Q_p \eta + \zeta^* Q_v \zeta + u^* R u)\,\mathrm{d}t$$

where Q_p, Q_v, and R are symmetric circulant matrices [9] whose first rows are given by the sequences $\{q_{p,m}\}, \{q_{v,m}\}$, and $\{r_m\}$ respectively. As usual, we demand $Q_p \geq 0, Q_v \geq 0$, and $R > 0$. We note that *any* spatially invariant quadratic cost functional for system (31), (32), that does not penalize products between positions and velocities, can be represented by (33).

The system (31), (32) has spatially invariant dynamics over a circle. This implies that the discrete Fourier transform

$$\hat{x}_k := \frac{1}{\sqrt{M}} \sum_{n=0}^{M-1} x_n \mathrm{e}^{-j\frac{2\pi n k}{M}}, \qquad k \in \{0, \ldots, M-1\}$$

can be used to convert analysis and quadratic design problems into those for a parameterized family of second order systems [3]. Using this, system (31), (32) and quadratic cost functional (33), respectively, transform to

$$\dot{\hat{\zeta}}_0 = \hat{u}_0 =: \hat{A}_0\hat{\phi}_0 + \hat{B}_0\hat{u}_0 \tag{34a}$$

$$\begin{bmatrix}\dot{\hat{\eta}}_k \\ \dot{\hat{\zeta}}_k\end{bmatrix} = \begin{bmatrix} 0 & \beta_k \\ 0 & 0\end{bmatrix}\begin{bmatrix}\hat{\eta}_k \\ \hat{\zeta}_k\end{bmatrix} + \begin{bmatrix}0\\1\end{bmatrix}\hat{u}_k \tag{34b}$$

$$=: \hat{A}_k\hat{\phi}_k + \hat{B}_k\hat{u}_k \quad k \in \{1, \ldots, M-1\}$$

and

$$J = \frac{\sqrt{M}}{2}\sum_{k=0}^{M-1}\int_0^\infty (\hat{\phi}_k^*(t)\hat{Q}_k\hat{\phi}_k(t) + \hat{r}_k\hat{u}_k^*(t)\hat{u}_k(t))\,\mathrm{d}t \tag{35}$$

where, $\hat{r}_k > 0$, for every $k \in \{0, \ldots, M-1\}, \hat{Q}_0 := \hat{q}_{v0} > 0$, and

$$\hat{Q}_k := \begin{bmatrix}\hat{q}_{pk} & 0 \\ 0 & \hat{q}_{vk}\end{bmatrix} \geq 0 \quad \beta_k := 1 - \mathrm{e}^{-j\frac{2\pi k}{M}}, \quad k \in \{1, \ldots, M-1\}.$$

Thus, the LQR problem (31)–(33) has been converted to a family of *uncoupled* LQR problems (34), (35) parameterized by $k \in \{0, \ldots, M-1\}$. The latter problem is easy to solve, and it yields the following optimal feedback, for every $k \in \{1, \ldots, M-1\}$:

$$\begin{aligned} \hat{u}_0 &= \hat{K}_{20}\hat{\zeta}_0 = -(\hat{q}_{v0}/\hat{r}_0)^{\frac{1}{2}} \\ \hat{u}_k &= \hat{K}_k\hat{\phi}_k = [\hat{K}_{1k}\ \hat{K}_{2k}]\begin{bmatrix}\hat{\eta}_k \\ \hat{\zeta}_k\end{bmatrix} \\ \hat{K}_{1k} &:= -\frac{\beta_k^*(\hat{q}_{pk}/\hat{r}_k)^{\frac{1}{2}}}{\left(2\left(1-\cos\frac{2\pi k}{M}\right)\right)^{\frac{1}{2}}} \\ \hat{K}_{2k} &:= -\left(\frac{\hat{q}_{vk}}{\hat{r}_k} + 2\left(2\frac{\hat{q}_{pk}}{\hat{r}_k}\left(1-\cos\frac{2\pi k}{M}\right)\right)^{\frac{1}{2}}\right)^{\frac{1}{2}} \end{aligned}$$

with the resulting closed-loop characteristic polynomial $f(s) := f_0(s)\cdots f_{M-1}(s)$, where

$$\begin{aligned} f_0(s) &= s + (\hat{q}_{v0}/\hat{r}_0)^{\frac{1}{2}} \\ f_k(s) &= s^2 + a_{1k}s + a_{0k} \\ a_{0k} &= -\beta_k\hat{K}_{1k} = \left(2\frac{\hat{q}_{pk}}{\hat{r}_k}\left(1-\cos\frac{2\pi k}{M}\right)\right)^{\frac{1}{2}} \\ a_{1k} &= -\hat{K}_{2k} = (\hat{q}_{vk}/\hat{r}_k + 2a_{0k})^{\frac{1}{2}} \\ &\qquad k \in \{1, \ldots, M-1\}. \end{aligned}$$

We now pose the question of whether it is possible to select design parameters $\hat{q}_{pk}, \hat{q}_{vk}$, and $\hat{r}_k$ that guarantee a prescribed "degree of stability" of the closed-loop system. In other words, we want to determine the conditions on $\hat{q}_{pk}, \hat{q}_{vk}$, and $\hat{r}_k$ to ensure uniform boundedness (away from the origin) of the roots of the closed-loop characteristic polynomial $f(s)$

$$\begin{aligned} |\lambda_{1k}| &\geq \alpha \quad k \in \{0, \ldots, M-1\}, \qquad \alpha > 0 \\ |\lambda_{2k}| &\geq \alpha, \qquad k \in \{1, \ldots, M-1\}, \quad \alpha > 0 \end{aligned} \tag{36}$$

where $\lambda_{10} := -\sqrt{\hat{q}_{v0}/\hat{r}_0}$. Since $f(s)$ is a product of at most second order terms, its roots can be explicitly computed. Thus, we can determine that (36) is satisfied if and only if

$$\frac{\hat{q}_{v0}}{\hat{r}_0} \geq \alpha^2 \quad \frac{\hat{q}_{vk}}{\hat{r}_k} \geq 2\alpha^2 \quad \frac{\hat{q}_{pk}}{\hat{r}_k} \geq \frac{\alpha^4}{2\left(1-\cos\frac{2\pi k}{M}\right)}$$

$k \in \{1, \ldots, M-1\}$, which implies the following lower bounds on the magnitudes of $\hat{K}_{1k}$ and $\hat{K}_{2k}$:

$$\hat{K}_{1k}^*\hat{K}_{1k} = \frac{\hat{q}_{pk}}{\hat{r}_k} \geq \frac{\alpha^4}{2\left(1-\cos\frac{2\pi k}{M}\right)} \qquad k \in \{1, \ldots, M-1\}$$

$$\hat{K}_{2k}^*\hat{K}_{2k} = \frac{\hat{q}_{vk}}{\hat{r}_k} + 2\left(2\frac{\hat{q}_{pk}}{\hat{r}_k}\left(1-\cos\frac{2\pi k}{M}\right)\right)^{\frac{1}{2}} \geq \begin{cases}\alpha^2 & k = 0 \\ 4\alpha^2 & k \in \{1, \ldots, M-1\}.\end{cases}$$

Thus, we have established that, in the formulation of [1], the uniform rate of convergence for all the vehicles can be secured by the appropriate selection of the state and control penalties. However, this comes at the price of increasing the control gains. For example, the lower bound

$$\hat{K}_{11}^*\hat{K}_{11} \geq \frac{\alpha^4}{2\left(1-\cos\frac{2\pi}{M}\right)}$$

increases unboundedly with the size of the platoon M. The reason for this is the existence of "almost uncontrollable" modes in (34b) for large M's. These modes introduce unfavorable scaling of $\hat{q}_{pk}/\hat{r}_k$ (that is, $\hat{K}_{1k}^*\hat{K}_{1k}$) with the number of vehicles in formation: for large platoons there are many k's for which $\hat{q}_{pk}/\hat{r}_k$ scales approximately as $\alpha^4 M^2$. Clearly, this requires the ratio between position and control penalties in the performance index to grow unboundedly in the limit of an infinite number of vehicles.

VI. Concluding Remarks

We have illustrated potential difficulties in the control of large or infinite vehicular platoons. In particular, shortcomings of previously reported solutions to the LQR problem have been exhibited. By considering the case of infinite platoons as the limit of the large-but-finite case, we have shown analytically how the aforementioned formulations lack stabilizability or detectability. We argued that the infinite case is a useful abstraction of the large-but-finite case, in that it explains the almost loss of stabilizability or detectability in the large-but-finite case, and the arbitrarily slowing rate of convergence toward desired formation observed in studies of finite platoons of increasing sizes. Finally, using the infinite platoon formulation, we showed how incorporating absolute position errors in the cost functional alleviates these difficulties and provides uniformly bounded rates of convergence.

The literature on control of platoons is quite extensive, and we have not attempted a thorough review of all the proposed control schemes here. However, it is noteworthy that the early work of [1], [2], [4], and [6] is widely cited, but to our knowledge these serious difficulties have not been previously pointed out in the literature.

As a further note, we point out that in [8] it was shown that imposing a uniform rate of convergence for all vehicles toward their desired trajectories may generate large control magnitudes for certain physically realistic initial conditions. Therefore, even though the formulation of an optimal control problem suggested in Section IV circumvents the difficulties with [1], [2], [4], and [6], additional care should be exercised in the control of vehicular platoons.

Acknowledgment

The first author would like to thank Prof. K. Åström and Prof. P. Kokotović for stimulating discussions. The authors would also like to thank M. Athans and W. Levine for a helpful discussion, and an anonymous reviewer and E. Jonckheere for their insightful comments.

References

[1] W. S. Levine and M. Athans, "On the optimal error regulation of a string of moving vehicles," *IEEE Trans. Autom. Control*, vol. AC-11, no. 3, pp. 355–361, Jul. 1966.

[2] S. M. Melzer and B. C. Kuo, "Optimal regulation of systems described by a countably infinite number of objects," *Automatica*, vol. 7, pp. 359–366, 1971.

[3] B. Bamieh, F. Paganini, and M. A. Dahleh, "Distributed control of spatially invariant systems," *IEEE Trans. Autom. Control*, vol. 47, no. 7, pp. 1091–1107, Jul. 2002.

[4] S. M. Melzer and B. C. Kuo, "A closed-form solution for the optimal error regulation of a string of moving vehicles," *IEEE Trans. Autom. Control*, vol. AC-16, no. 1, pp. 50–52, Feb. 1971.

[5] U. Grenander and G. Szegö, *Toeplitz Forms and Their Applications*. New York: Chelsea, 1984.

[6] K. C. Chu, "Decentralized control of high-speed vehicular strings," *Transport. Sci.*, vol. 8, no. 4, pp. 361–384, Nov. 1974.

[7] K. Zhou, J. C. Doyle, and K. Glover, *Robust and Optimal Control*. Upper Saddle River, NJ: Prentice-Hall, 1996.

[8] M. R. Jovanović, J. M. Fowler, B. Bamieh, and R. D'Andrea, "On avoiding saturation in the control of vehicular platoons," in *Proc. 2004 Amer. Control Conf.*, Boston, MA, 2004, pp. 2257–2262.

[9] R. W. Brockett and J. L. Willems, "Discretized partial differential equations: Examples of control systems defined on modules," *Automatica*, vol. 10, pp. 507–515, 1974.

Mihailo R. Jovanović (S'00–M'05) was born in Arandjelovac, Serbia. He received the Dipl. Ing. and M.S. degrees, both in mechanical engineering, from the University of Belgrade, Belgrade, Serbia, in 1995 and 1998, respectively, and the Ph.D. degree in mechanical engineering from the University of California, Santa Barbara, in 2004.

He was a Visiting Researcher with the Department of Mechanics, the Royal Institute of Technology, Stockholm, Sweden, from September to December 2004. He joined the Department of Electrical and Computer Engineering, the University of Minnesota, Minneapolis, as an Assistant Professor in December 2004. His primary research interests are in modeling, analysis, and control of spatially distributed dynamical systems.

Bassam Bamieh (S'82–M'91–SM'04) received the B.S. degree in electrical engineering and physics from Valparaiso University, Valparaiso, IN, in 1983, and the M.Sc. and Ph.D. degrees from Rice University, Houston, TX, in 1986 and 1992, respectively.

During 1991–1998, he was with the Department of Electrical and Computer Engineering and the Coordinated Science Laboratory, the University of Illinois at Urbana-Champaign. He is currently a Professor in the Mechanical Engineering Department, the University of California, Santa Barbara, which he joined in 1998. His current research interests are in distributed systems, shear flow turbulence modeling and control, quantum control, micro-cantilevers modeling and control, and optical actuation via optical tweezers.

Dr. Bamieh is a past recipient of the AACC Hugo Schuck Best Paper award, the IEEE Control Systems Society Axelby Outstanding Paper Award, and a National Science Foundation CAREER Award. He is currently an Associate Editor of *Systems and Control Letters*.